Enhanced Carbon Sequestration in Alkaline Lakes through Recycled CO_2 Utilization by Diatoms

Dinggui Wu[1,2], Qingfeng Zhao[1], Siyu Huang[3], Yuxin He[1], Jinglu Wu[4], Yongge Sun[1]*

[1]Organic Geochemistry Unit, School of Earth Sciences, Zhejiang University, Hangzhou 310027, China

[2]College of Oceanography, Hohai University, Nanjing210024, China

[3]College of Environment and Resources, Guangxi Normal University, Guilin 541004, China

[4]State Key Laboratory of Lake Science and Environment, Nanjing Institute of Geography and Limnology, Chinese Academy of Sciences (CAS), Nanjing 210008, China.

*Corresponding author. Yongge Sun (ygsun@zju.edu.cn)

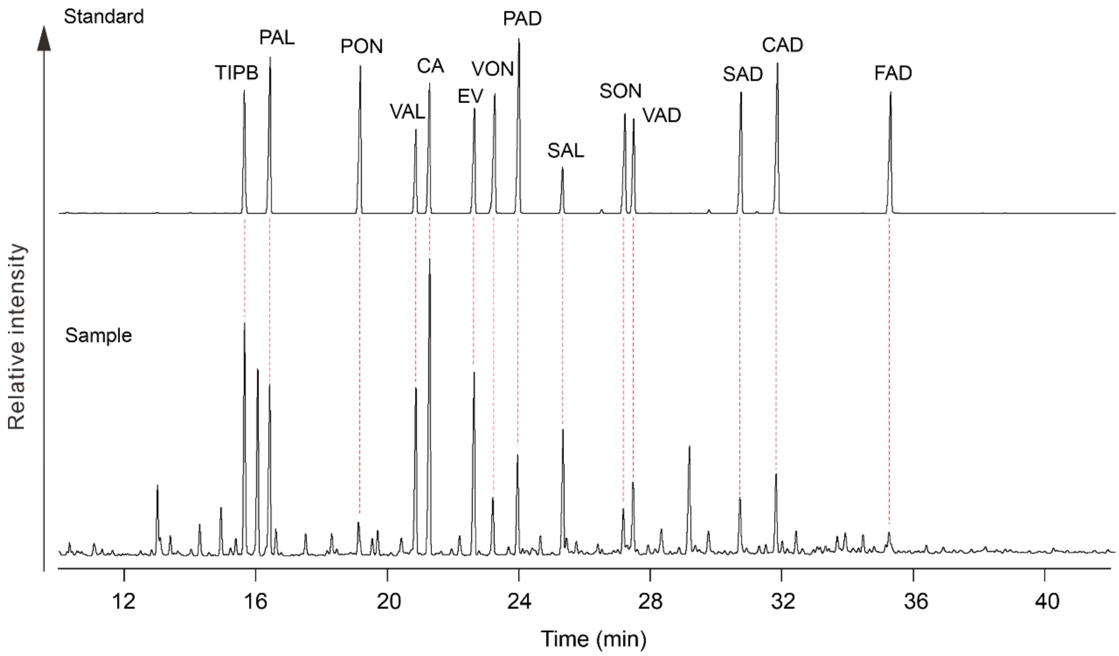

Fig. S1. Gas chromatograms of lignin-derived phenols in surface sediments from the Lake Haixihai compared with those of the standard compounds. Peaks from left to right are identified as 1,3,5-triisopropylbenzene (TIPB), *p*-hydroxybenzaldehyde (PAL), *p*-hydroxyacetophenone (PON), vanillin (VAL), trans-cinnamic acid (CA), ethyl vanillin (EV), acetovanillone (VON), *p*-hydroxybenzoic acid (PAD), syringaldehyde (SAL), acetosyringone (SON), vanillic acid (VAD), syringic acid (SAD), *p*-coumaric acid (CAD), and ferulic acid (FAD).

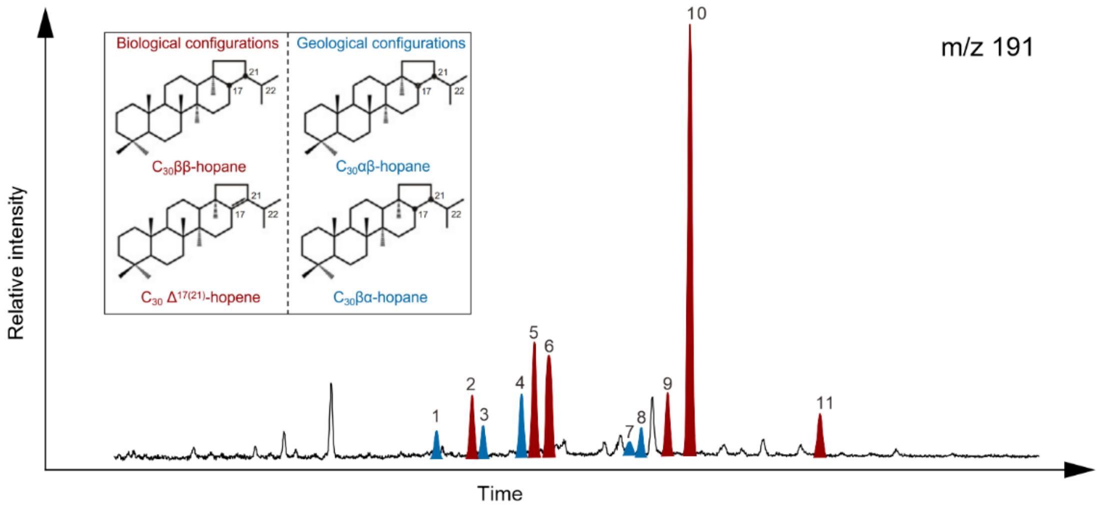

Fig. S2. Mass fragmentograms of triterpanes (m/z 191) in surface sediments from Lake Haixihai. 1: C_{29} αβ-hopane, 17α(H), 21β(H)-30-norhopane. 2: hop-17(21)-ene. 3: C_{29}βα-hopane, 17β(H), 21α(H)-30-normoretane. 4: C_{30}αβ-hopane, 17α(H), 21β(H)-hopane. 5: hop-13(18)-ene. 6: C_{29}ββ-hopane, 17β(H), 21β (H)-30-norhopane. 7: C_{31}αβ-hopane, 17α(H), 21β(H)-homohopane (S). 8: C_{31}αβ-hopane (R), 17α(H), 21β(H)-homohopane (R). 9: C_{30}ββ-hopane, 17β(H), 21β(H)-hopane; 10: 17β(H)-hop-22(29)-ene (diploptene). 11: C_{31}ββ-hopane, 17β(H), 21β(H)-homohopane.

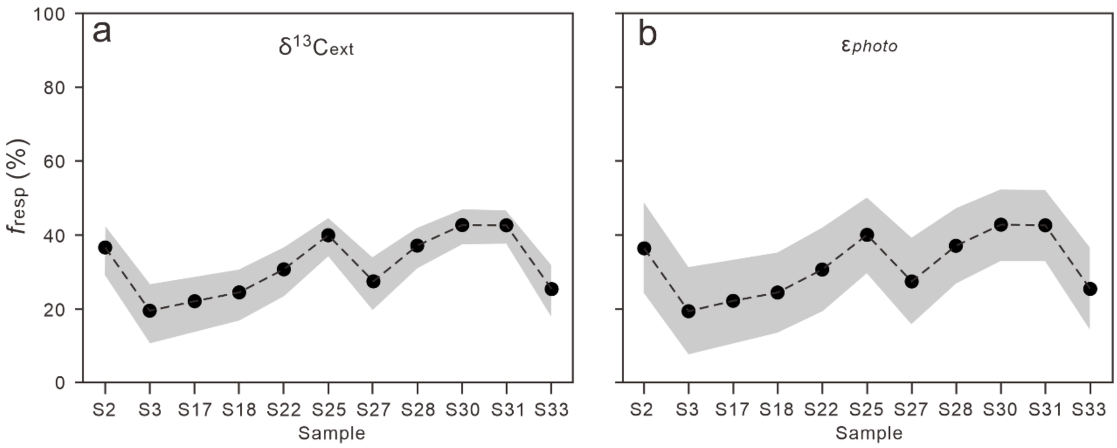

Fig. S3. Sensitivity of the estimated fraction of respired CO_2(aq) assimilated by diatoms (fresp) to model parameters. Shown are Monte Carlo sensitivity analyses for (a) the isotopic composition of the external inorganic carbon endmember ($\delta^{13}C_{ext}$), and (b) the effective photosynthetic fractionation factor (ε_{photo}). For each sensitivity test, one parameter was systematically varied across its prescribed range while the other two were randomly sampled within their respective ranges. Reported f_{resp} values correspond to medians across all samples, with 95% confidence intervals derived from the ensemble of simulations. Solid dark red lines indicate median values of f_{resp} across all samples, whereas shaded light red envelopes denote the 95% uncertainty intervals derived from Monte Carlo simulations.

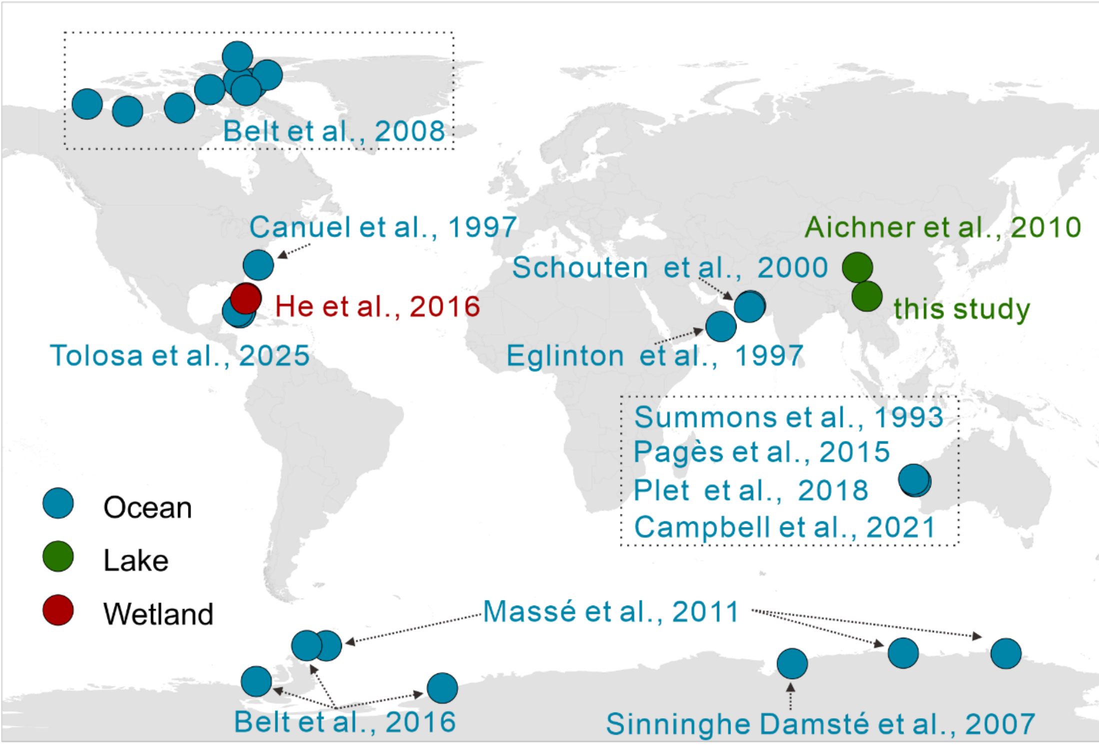

Fig. S4. Locations of the study sites compiled from the literature. Blue circles represent marine case studies, green circles represent lake case studies, and red circles represent wetland case studies.

Table S1. Compilation of stable carbon isotopic data of C_{25} HBIs from different aquatic systems reported in the literature.

Research region	Aquatic system	Sample name	Longitude (°)	Altitude (°)	C_{25}HBI type	$\delta^{13}C$	Reference
Arabian Sea	Ocean	Site 451	66.06	23.68	C25:0	-23.3	Schouten et al., 2000
		Site 453	65.75	23.26	C25:0	-21.7	
Hamelin Pool	Ocean	NA	114.09	-26.22	C25:0	-11	Summons et al., 1993
		NA			C25:1	-12	
		NA			C25:2	-12.8	
Arabian Sea	Ocean	Core 6BC	57.51	17.81	C25:2	-19.9	Eglinton et al., 1997
Outer Banks of North Carolina	Ocean	CLB surface waters SPM 13 Sept 91	-77.10	34.62	C25:2	-20.32	Canuel et al., 1997
		CLB surf sediments 27 Feb 88			C25:2	-22.2	
		CLB surf sediments 2 Oct 88			C25:2	-19.9	
Arctic	Ocean	NOW-1	-78.75	75.67	C25:1	-16.9	Belt et al., 2008
		NOW-2	-82.97	76.18	C25:1	-16.3	
		ARC-1 0-1CM	-74.53	77.84	C25:1	-21.7	
		ARC-1 29-30CM			C25:1	-19.7	
		ARC-2 0-1CM	-80.68	73.97	C25:1	-20.2	
					C25:2	-42.2	
		ARC-2 29-30CM			C25:1	-20.8	
		ARC3 36-37CM	-91.23	74.16	C25:1	-18.5	
					C25:2	-18.2	
		ARC3 59-60 CM			C25:1	-18.7	
		ARC3 109-110 CM			C25:1	-18.4	
		ARC3 133-134 CM			C25:1	-17.5	
		ARC3 230-231 CM			C25:1	-18.9	
		ARC3 333-334 CM			C25:1	-18.6	
		ARC3 437-438 CM			C25:1	-19.0	
		ARC4 32-33 CM	-100.02	69.90	C25:1	-18.7	
					C25:2	-17	
		ARC4 61-62 CM			C25:1	-23.2	
		ARC4 469-470 CM			C25:1	-14.0	
		ARC5 0-1CM	-115.14	69.16	C25:1	-21.2	
		ARC5 129-130CM			C25:1	-16.9	
		ARC5 408-409CM			C25:1	-18.4	
		ARC-6	-126.91	70.79	C25:1	-23.2	
		Sediment trap			C25:1	-19.6	
		Sea ice			C25:1	-22.3	
Batabanó Gulf	Ocean	site-1	-82.22	22.62	C25:1	-16.0	Tolosa et al., 2025
		site-3	-82.23	22.23	C25:1	-9.7	
		site-4	-82.43	22.10	C25:1	-12.0	

		site-5	-82.47	22.90	C25:1	-10.9	
		site-6	-82.47	21.69	C25:1	-12.5	
		site-9	-83.17	83.17	C25:1	-15.0	
		site-14	-83.17	22.16	C25:1	-10.8	
Ellis Fjord	Ocean	2-3CM	78.23	-68.60	C25:2	-9.1	Sinninghe Damsté et al., 2007
		6-7CM			C25:2	-9.4	
Antarctic	Ocean	Weddell Sea 3	-57.33	-64.73	C25:2	-8.5	Massé et al., 2011
		O'Brien Bay 1	110.54	-66.29	C25:2	-5.7	
		MD130-MC02	140.42	-66.40	C25:2	-17.8	
Antarctic	Ocean	Marguerite Bay (WAP)	-63.02	-64.70	C25:2	-15.0	Belt et al., 2016
		SE Weddell Sea	-23.55	-74.21	C25:2	-13.5	
		The northern AP	-77.70	-72.61	C25:2	-14.4	
Shark Bay	Ocean	Smooth mat	113.85	-26.37	C25:1	-12.6	Plet et al., 2018
Shark Bay	Ocean	Black sludge	114.21	-26.37	C25:1	-17.19	Campbell et al., 2021
					C25:0	-16.6	
		Outer cobble section	114.21	-26.37	C25:1	-15.1	
					C25:0	-16.6	
		Inner cobble section	114.21	-26.38	C25:1	-14.6	
		Sludge between columns	114.21	-26.38	C25:1	-14.3	
					C25:0	-15.0	
		Tufted mat	114.21	-26.38	C25:1	-13.6	
					C25:0	-13.7	
		Smooth mat	114.20	-26.38	C25:1	-13.9	
					C25:0	-14.4	
		Ooze over sand	114.20	-26.38	C25:1	-13.9	
					C25:0	-14.4	
Shark Bay	Ocean	microbial mat	113.54	-25.70	C25:1	-15.2	Pagès et al., 2015
Lake Haixihai	Lake	S2	99.96	26.28	C25:2	-22.7	this study
		S27			C25:2	-20.9	
		S3			C25:2	-18.9	
		S33			C25:2	-20.7	
		S17			C25:2	-19.7	
		S18			C25:2	-20.6	
		S22			C25:2	-21.8	
		S25			C25:2	-25.3	
		S31			C25:2	-26.8	
		S28			C25:2	-24.5	
		S30			C25:2	-26.7	
Lake Koucha	Lake	0 cm	97.20	34.00	C25:2	-21	Aichner et al., 2010
		23 cm			C25:2	-22.7	
		76 cm			C25:2	-22.9	
		96 cm			C25:2	-21.1	
		116 cm			C25:2	-19.3	

		124 cm			C25:2	-21.1	
		136 cm			C25:2	-24.6	
		156 cm			C25:2	-21.1	
		192 cm			C25:2	-20.9	
		204 cm			C25:2	-20.7	
		220 cm			C25:2	-19.3	
		253 cm			C25:2	-22.5	
Everglades National Park	Wetland	WCA3 periphyton	-80.62	25.83	C25:2	-39.7	He et al., 2016
					C25:3	-40.0	
		WCA3 ridge floc			C25:2	-39.3	
					C25:3	-39.0	
		WCA3 slough floc			C25:2	-39.7	
					C25:3	-39.5	
		WCA3 surface soil			C25:2	-38.5	
					C25:3	-39.1	
		SRS2 floc	-80.80	25.53	C25:2	-38.9	
					C25:3	-39.3	

References

Aichner, B., Wilkes, H., Herzschuh, U., Mischke, S., & Zhang, C.J. 2010. Biomarker and compound-specific $\delta^{13}C$ evidence for changing environmental conditions and carbon limitation at Lake Koucha, eastern Tibetan Plateau. *Journal of Paleolimnology* 43: 873-899. https://doi.org/10.1007/s10933-009-9375-y.

Belt, S.T., Massé, G., Vare, L.L., Rowland, S.J., Poulin, M., Sicre, M.-A., Sampei, M., & Fortier, L. 2008. Distinctive ^{13}C isotopic signature distinguishes a novel sea ice biomarker in Arctic sediments and sediment traps. *Marine Chemistry* 112: 158-167. https://doi.org/https://doi.org/10.1016/j.marchem.2008.09.002.

Belt, S.T., Smik, L., Brown, T.A., Kim, J.H., Rowland, S.J., Allen, C.S., Gal, J.K., Shin, K.H., Lee, J.I., & Taylor, K.W.R. 2016. Source identification and distribution reveals the potential of the geochemical Antarctic sea ice proxy IPSO25. *Nature Communications* 7: 12655.

https://doi.org/10.1038/ncomms12655.

Campbell, M.A., Coolen, M.J.L., Visscher, P.T., Morris, T., & Grice, K. 2021. Structure and function of Shark Bay microbial communities following tropical cyclone Olwyn: A metatranscriptomic and organic geochemical perspective. *Geobiology* 19: 642-664. https://doi.org/https://doi.org/10.1111/gbi.12461.

Canuel, E.A., Freeman, K.H., & Wakeham, S.G. 1997. Isotopic compositions of lipid biomarker compounds in estuarine plants and surface sediments. *Limnology and Oceanography* 42: 1570-1583. https://doi.org/https://doi.org/10.4319/lo.1997.42.7.1570.

Eglinton, T.I., Benitez-Nelson, B.C., Pearson, A., McNichol, A.P., Bauer, J.E., & Druffel, E.R. 1997. Variability in radiocarbon ages of individual organic compounds from marine sediments. *Science* 277: 796-799.

He, D., Simoneit, B.R.T., Xu, Y.P., & Jaffé, R. 2016. Occurrence of unsaturated C25 highly branched isoprenoids (HBIs) in a freshwater wetland. *Organic Geochemistry* 93: 59-67. https://doi.org/10.1016/j.orggeochem.2016.01.006.

Massé, G., Belt, S.T., Crosta, X., Schmidt, S., Snape, I., Thomas, D.N., & Rowland, S.J. 2011. Highly branched isoprenoids as proxies for variable sea ice conditions in the Southern Ocean. *Antarctic Science* 23: 487-498. https://doi.org/10.1017/S0954102011000381.

Pagès, A., Grice, K., Welsh, D.T., Teasdale, P.T., Van Kranendonk, M.J., & Greenwood, P. 2015. Lipid Biomarker and Isotopic Study of Community Distribution and Biomarker Preservation in a Laminated Microbial Mat from

Shark Bay, Western Australia. *Microbial Ecology* 70: 459-472. https://doi.org/10.1007/s00248-015-0598-3.

Plet, C., Pagès, A., Holman, A.I., Madden, R.H.C., & Grice, K. 2018. From supratidal to subtidal, an integrated characterisation of Carbla Beach shallow microbial mats (Hamelin Pool, Shark Bay, WA): Lipid biomarkers, stable carbon isotopes and microfabrics. *Chemical Geology* 493: 338-352. https://doi.org/https://doi.org/10.1016/j.chemgeo.2018.06.010.

Schouten, S., Hoefs, M.J.L., & Sinninghe Damsté, J.S. 2000. A molecular and stable carbon isotopic study of lipids in late Quaternary sediments from the Arabian Sea. *Organic Geochemistry* 31: 509-521. https://doi.org/https://doi.org/10.1016/S0146-6380(00)00031-0.

Sinninghe Damsté, J.S., Rijpstra, W.I.C., Coolen, M.J.L., Schouten, S., & Volkman, J.K. 2007. Rapid sulfurisation of highly branched isoprenoid (HBI) alkenes in sulfidic Holocene sediments from Ellis Fjord, Antarctica. *Organic Geochemistry* 38: 128-139. https://doi.org/https://doi.org/10.1016/j.orggeochem.2006.08.003.

Summons, R.E., Barrow, R.A., Capon, R.J., Hope, J.M., & Stranger, C. 1993. The structure of a new C25 isoprenoid alkene biomarker from diatomaceous microbial communities. *Australian Journal of Chemistry* 46: 907-915. https://doi.org/10.1071/ch9930907.

Tolosa, I., Mesa-Albernas, M., & Alonso-Hernández, C.M. 2025. Assessing the sources of organic matter in sediments from the Gulf of Batabanó (Cuba) using stable isotopes, aliphatic and polycyclic aromatic hydrocarbons.

Continental Shelf Research 285: 105405.

https://doi.org/https://doi.org/10.1016/j.csr.2025.105405.